BENDING INDUCED VERTICAL OSCILLATIONS DURING SEISMIC RESPONSE OF RC BRIDGE PIERS

Giulio RANZO[1], Marco PETRANGELI[2] And Paolo E PINTO[3]

SUMMARY

The paper presents a numerical investigation on the behaviour of reinforced concrete bridge piers subjected to horizontal seismic input. Scope of the investigations is to quantify the phenomenon of bending-induced axial vibrations. The results of a set of analyses conducted on single column bent systems indicate that flexural cracking produces, in fact, significant axial vibrations. Quantification of the effects related to this phenomenon can be determinant for the seismic assessment of existing bridges as well as for the design of new bridges. Likewise, performance and design forces of bearings and other anti-seismic devices can be estimated with more accuracy, based on the expected level of combined vertical and horizontal acceleration response on decks. Shear resisting mechanisms should also be sensitive to these vibrations and shear failure anticipated when a reduction in the axial contribution to the section shear capacity occurs. A tentative equation for the prediction of this flexural-induced vertical acceleration component is proposed based on simplified section kinematics and elastic impact analysis.

INTRODUCTION

The field evidence [Ono et al. ,1996] of the damaging effects due to axial vibrations in vertical members of RC structures during past earthquakes, has attracted the attention of various authors. While the effects of vertical ground motion components on buildings and bridges [Papazoglou et al. ,1996][Elnashai et al. ,1997] have been studied, no attention has been dedicated so far to the bending induced vertical accelerations in RC members subjected to inelastic oscillations. This type of vertical oscillations is independent of the vertical ground motion input and can induce vertical accelerations that are comparable to the horizontal ones [Petrangeli et al. ,1997] .

Scope of the present work is to quantify these bending induced vertical oscillations due to the rocking mechanism of r.c. bridge piers, with particular reference to systems in which the deck is made of multiple girders supported by large cap beams. In this kind of structures, very frequent in European and Japanese highway networks, these vibrations may have a significant effect on the general structural performance. The frequency content and magnitude of the vertical motion associated with this effect is analyzed for different structures, with different natural periods. Consequences on the performance of bearings is also investigated. A simplified model, based on the cracked section kinematics, is developed to predict the magnitude of bending-induced axial accelerations.

THE ANALYSED STRUCTURES : GEOMETRY AND DIMENSIONING

Three different structures, meant to be representative of typical prestressed concrete viaducts in seismic regions, have been analysed. The three structures have the same *30m* span superstructure and different pier heights: *6*, *12* and *18m* respectively. Each analysed structure is supposed to be part of a viaduct made of a sequence of equal

[1] *1 PhD Student, University of Rome "La Sapienza", Rome, Italy – Email : granzo@dsg.uniroma1.i*
[2] *Assistant Professor , University of Chieti "G.D'Annunzio", Pescara, Italy*
[3] *Professor of Earthquake Engineering, University of Rome "La Sapienza", Rome, Italy*

spans, simply supported on piers of similar heights. The analysis of the seismic response of these structures in the transverse direction is then carried out on a 2D schematisation, taking into consideration one pier only with two half spans each side.

The superstructure, with a total platform width of *15.7m*, is made of a *0.25m* reinforced concrete slab connecting four prestressed concrete girders as shown in Fig.1. This deck configuration requires a *11.5m* wide cap beam, in order to seat four bearings with a centre to centre distance of *3.5m*. The weight of one span has been assumed equal to *6000kN*, therefore a vertical load of *1500kN* acts on each bearing support. An additional weight of *600 kN* has been considered to account for the cap beam.

Dimensioning of the pier cross section has been carried out so as to obtain a normalised axial load $P/f_c^{'}A_g = 0.1$ under self weight alone, as typical for this kind of structures ($f_c^{'}$ is the unconfined concrete compression strength and A_g is the area of the gross section). The flexural capacity of the pier cross section, reflecting the actual situation of most existing viaducts, has been dimensioned according to allowable stress criteria. For each structure, the design moment is computed based on a constant response spectrum of *0.1g*. The required flexural capacities are therefore proportional to the pier height since the total mass is roughly the same for the three cases; the base bending moments are computed on a cantilever scheme, neglecting the influence of deck torsional inertia and cap beam flexibility. The same hollow cross-section has been adopted in the three cases with different amount of longitudinal reinforcing steel ρ_l. Table 2 summarises the main design characteristics.

The first yield moment M_y (bending moment at first yield of longitudinal rebars) and the nominal moment M_n (defined here as the bending moment at 5 times yield curvature) are indicated to conventionally define the mechanical properties. Shear dimensioning of the three structures is omitted since the investigations are focused on axial-flexural coupling, however it is assumed that adequate shear reinforcement is provided to ensure a flexural dominant response when large inelastic displacements occur.

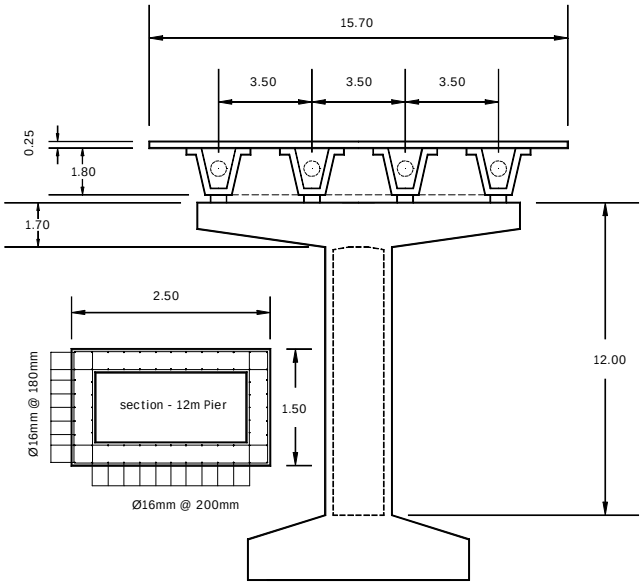

Figure 1 – Geometry of the analysed structures

Tab. 1 Results of modal analyses

Pier Height [m]	ρ_l [%]	M_y [kNm]
6	0.35	9667
12	0.7	12204
18	1.0	14090

Tab. 2 – Pier properties

Pier height [m]	Mode number	Mass % X dir.	Mass % Y dir.	T [sec.]
6	1	51.0	-	0.583
6	2	48.0	-	0.123
6	3	-	76.0	0.070
12	1	79.9	-	1.190
12	2	20.1	-	0.232
12	3	-	90	0.090
18	1	89.9	-	1.960
18	2	10.1	-	0.303
18	3	-	95	0.104

Before analysing the nonlinear behaviour of these structures it is interesting to see the results of the modal analysis. Natural frequencies and participating masses in x and y direction and modal shapes are indicated in table 2 and fig.2.

When these structures are modelled with realistic flexibility for the cap beam and both vertical and rotational masses are included to account for the vertical loads of the superstructure acting on the bearing supports, higher

modes significantly influence the global behaviour. Especially in the case of the short pier, a significant percentage of horizontal modal mass is found in the second mode, which is of the double bending type. Concrete cracking will therefore take place in the top and bottom sections, possibly increasing the hammering effect at bending reversal. In the *12* and *18* metre piers instead, the deck rotational inertia is less significant when compared to the pier flexibility. The pier deforms mainly in simple bending with concrete cracking located at pier base only.

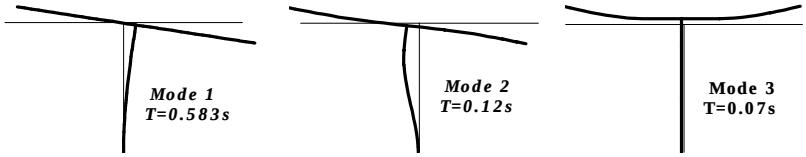

Figure 2 – Modal shapes

THE NUMERICAL MODELS FOR NON-LINEAR TIME-HISTORY ANALYSES

The three structures have been modelled by using a flexibility-based fibre beam element developed by the authors [Petrangeli et al. ,1999]. Each pier has been modelled using two fibre beam elements with three, four and five integration Gauss points (monitoring sections) for the *6, 12* and *18* metres piers respectively. The number of integration points has been selected in order to attain the same numerical precision in integrating the longitudinal strain field in the three structures, while maintaining the same tributary length to each integration point.
The pier cap has been modelled using linear elastic elements with equivalent mechanical properties. Constitutive models for concrete and reinforcing steel adopt state-of-the-art uniaxial stress-strain relationships based on the work of Mander [Mander et al. ,1988] and [Menegotto et al.,1977] respectively (see also fig. 5 and 6). In the concrete model, a crack-bridging branch has been introduced, providing a smooth transition between the tensile and the compression branches. This feature was required in order to avoid an overestimation of the impulsive component of vertical acceleration at crack closure as a result of the abrupt transition between the zero stiffness, zero stress cracked state and the reloading branches to compression.

Mechanical properties of the steel have been assumed as follows: yield strength = *400 MPa*, ultimate strength = *570 MPa*, Young's modulus = *200000 MPa*, ultimate strain = *0.10*. Mechanical properties of the concrete are: unconfined strength = *35 MPa*, confined strength = *42 MPa*, strain at ultimate stress = *0.0035*, Young's modulus = *30000 MPa*, tensile strength = *2.5 MPa*, fracture energy = *0.1 kN/m*.

The deck horizontal mass (*600t*) has been placed in one node only (as indicated in fig.3) to avoid axial (horizontal) vibrations in the pier cap beam; vertical masses have been placed instead at each beam support (*150t* each) and at pier top (*60t*). The masses of the superstructure are rigidly connected to the cap beam.
The first mode natural frequencies computed with modal analysis have been used to quantify the viscous component of the structural damping. A viscous damping, in addition to the hysteretic one, has been considered in fact by means of a mass proportional damping factor *C*, where, for elastic systems, $C = 2\xi\omega m$ with *m* the mass, ξ the percentage of critical damping and ω the circular frequency. A value of *3%* of critical damping has been assumed in our case to be representative of all viscous damping components acting within the elastic structural response.

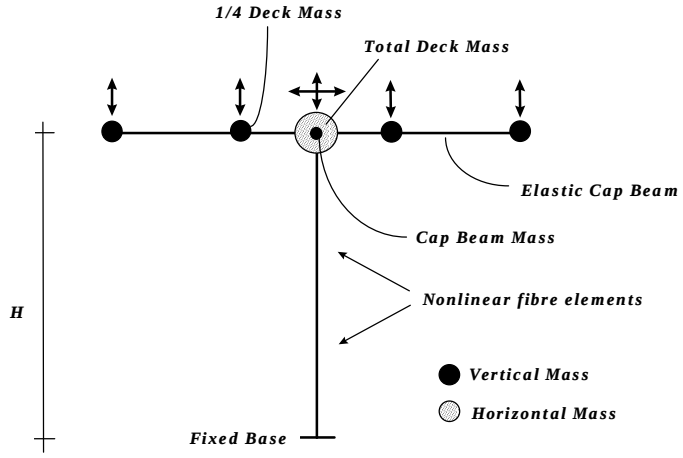

Figure 3 – Numerical model

RESULTS OF NON-LINEAR ANALYSES

A set of non-linear time-history analyses using the general purpose F.E. code FIBER has been performed using an accelerogram compatible with the EC8 response spectrum with *PGA=0.35g* as horizontal ground motion

input. The vertical component has been purposely ignored in a first stage, while it has been included in a second set of analyses to evaluate the coupling effect on the pier axial response.

Under the imposed horizontal ground motion, large inelastic deformations occur in the three structures. In all cases a plastic hinge forms at pier base, where longitudinal reinforcing bars reach (for the *6m* pier) a maximum strain of approximately *2.0%*. Maximum base shears are *2500kN, 1250kN* and *980kN* for the *6m, 12m* and *18m* pier respectively. Moment curvature cycles at pier base are plotted in fig.4. In the same graphs the corresponding axial force time history is also reported. The largest ductilities are found for the *6m* pier with a curvature ductility $\mu_\phi = 8 \div 9$. For this pier, the inflection point is located at *0.54H* (with *H* full height of the pier), while for the *12m* and *18m* is *0.66H* and *0.69H* respectively. Note that the maximum axial force fluctuations are found for the *6m* pier (*+58%* of additional compression and *-35%* in axial force reduction). None of the piers experienced steel yielding in the top section below the pier cap beam. Concrete and steel stress-strain histories for the base section of the *6m* pier are plotted in fig. 5 and 6.

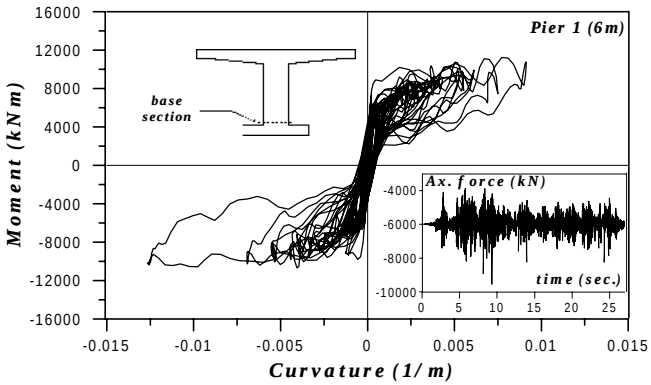

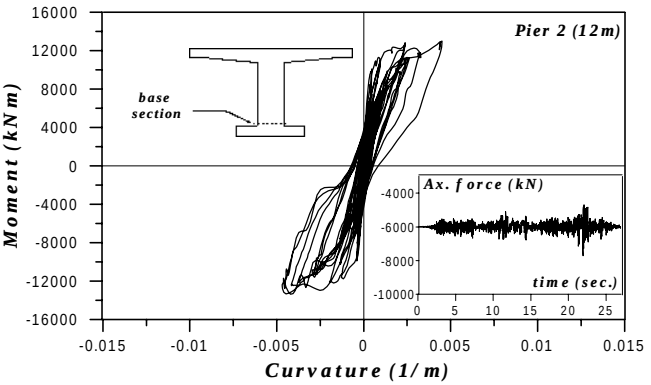

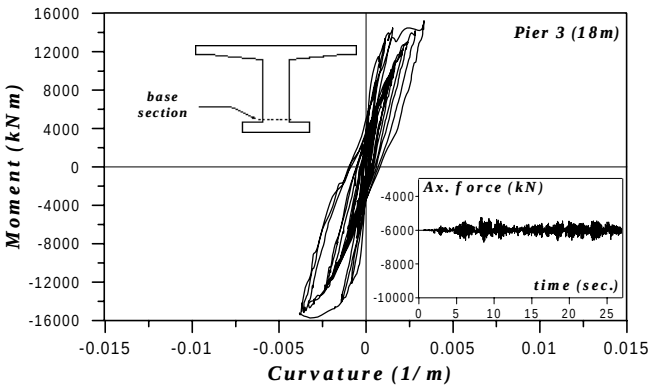

In the *6m* pier a global displacement ductility of about *5.0* is reached, compared to *2.5* and *2.0* in the *12m* and *18m* pier respectively. This remarkable difference in global damage is due to the inappropriate strength provided by the allowable stress design criterion and to the flat design spectrum adopted *(0.1g)*. However, this result reflects the actual situation on existing viaducts where squat piers tend to have light longitudinal reinforcement ratios. Maximum displacement drifts are in a range of *0.75%* to *1%* of the pier height. Maximum vertical displacements at external bearing locations are insensitive to the pier height and are always around *0.05m*.

The maximum response of the three structures is summarised in fig.7 (the *5%* damping elastic response spectrum of the accelerogram used in the analyses is also reported). Maximum accelerations at bearing locations are indicated for each structure as a function of their fundamental elastic flexural period. It can be seen that in the proposed examples, the deck horizontal maximum acceleration does not vary significantly with pier height while the vertical acceleration does, due to varying axial/flexural period ratio as well as cap beam width/pier height ratio.

As anticipated before, vertical acceleration

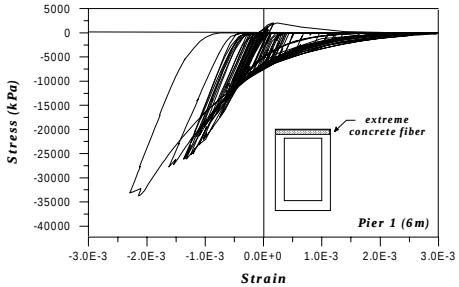

Figure 5 - Concrete

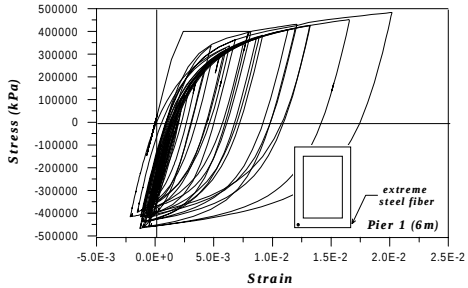

Figure 6- Steel

response is particularly high for the squat pier, where a peak value of *0.9g* is found at external bearing location. Generally, bending-induced vertical accelerations decrease with increasing pier height as also confirmed by other analyses. Vertical acceleration of the outer bearings includes in fact also a "geometric" component due to the rotational acceleration of the pier cap beam itself. This component obviously decreases with decreasing cap beam width/pier height ratio. The distribution of the vertical acceleration along the cap beam from pier top to the external bearing location can be easily derived from the graphs of fig.7.

The plots of fig.8 show the acceleration response spectra (with *5%* damping) of the horizontal and vertical deck motion recorded at each bearing location and at pier top. The ground motion spectrum is plotted for comparison. These spectra provide an idea of the frequency content and magnitude of the structural response. Their values for *T=0* correspond to the maximum accelerations plotted in fig.7 which are the ones to be used to evaluate the maximum vertical and horizontal force transmitted between deck and piers. In fig.7, the peak below *0.2 sec*. at the outer bearing location is clearly due to the selective amplification of the first vertical vibration mode of the pier (mode 3 in tab2). It can be seen that the response spectra of the vertical accelerations tend to be more concentrated in a narrow band of frequencies as the pier flexural period increases, while those of horizontal accelerations tend instead to have a constant level of response (i.e. frequency independent) around *0.75g.*

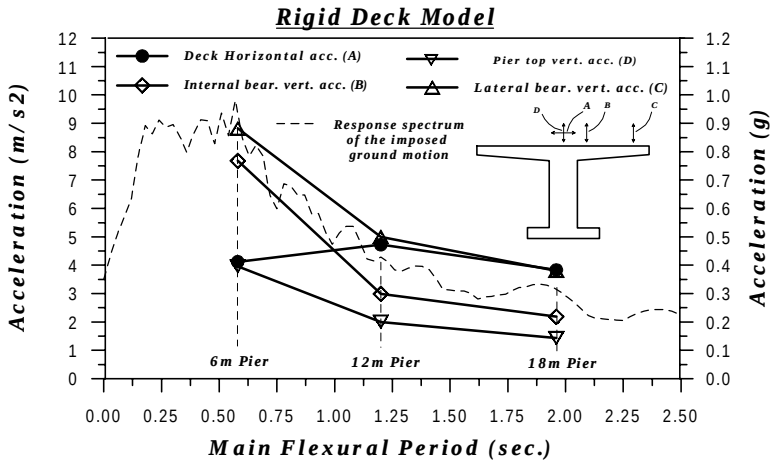

Figure 7 – Maximum response

It can be noted from the results discussed above that on external bearings vertical acceleration response is equal or greater (up to a factor of *2* for the *6m* pier) than the horizontal one. With the ratio between vertical and horizontal force on bearings (R_v/H) falling to such low values, unseating phenomena are likely to occur. The most significant examples of these low values occurred during the analysis are reported in table 3 for both internal and external bearing in the *6m* pier. Note that the vertical reaction under self weight alone is equal to *1500kN*. Response at *8.22 sec.* shows instead a case where the maximum vertical reaction of the bearings is nearly twice the static one. During the analysis the external bearing experiences a minimum ratio between vertical reaction R_v and shear force *H* equal to *0.65*, while the internal bearing has a minimum value of *2.26*.

Tab. 3 - Forces on bearings during earthquake response

	External Bearing		*Internal Bearing*	
Time (sec.)	**Shear**	**R_v(kN)**	**Shear**	**R_v(kN)**
5.23	-469	305	-469	1119
8.22	43	2639	43	1932
8.26	-572	556	-572	1500

If the effect of the vertical ground motion component is now introduced, a quantification of the relative importance of the two different sources of axial vibrations can be made.

The analyses carried out above were repeated again with inclusion of a vertical motion with peak ground acceleration equal to *2/3* of horizontal peak acceleration. This ground motion component is still compatible with the EC8 response spectrum and has the same duration and starting time step of that of horizontal motion. In these analyses the two sources of axial vibrations are therefore taken into account and their effects appear combined. The values are in all cases larger than the corresponding ones in fig.7, where the ground vertical acceleration is absent, but the order of magnitude does not change. In other words, from the 'spot' cases examined it would seem that the predominant contribution to the vertical response accelerations comes from the rocking mechanism, not from the vertical acceleration input.

SIMPLE MECHANICAL MODEL FOR AXIAL VIBRATIONS

An attempt to establish a closed form approximate relationship between these axial vibrations and the pier

flexural response will be presented herein. The main assumption is that cracked sections can be treated as rigid bodies during their motion induced by flexural response. In this idealisation the sections rotate about a point that coincides with the position of the neutral axis. The impact of the sections during bending reversal will be assumed elastic with initial conditions (i.e. values of velocity and acceleration) found from the rigid body motion assumption.

Assuming that plane sections remain plane the following relation holds between the curvature χ and axial elongation ε_p for a RC section:

$$\varepsilon_p = |\chi| \left(k - \frac{1}{2} \right) d \qquad (1)$$

where k is a scalar parameter ($0 \le k \le 1$) defining the neutral axis depth $(1-k)d$. Let us now assume the flexural response of a generic section be described by a simple sinusoidal function as follows:

$$\chi(t) = \chi^{max} \sin\left(\frac{2\pi t}{T_f} \right) \qquad (2)$$

with T_f being the predominant flexural period of the pier. The section axial deformation, according to (1), can therefore be written:

$$\varepsilon_p(t) = \chi^{max} \left| \sin\left(\frac{2\pi t}{T_f} \right) \right| \left(k - \frac{1}{2} \right) d \qquad (3)$$

where the absolute value of the sinusoidal function is taken since the axial elongation is always positive.

In order to obtain simple expressions for the velocity and the acceleration of the axial strain (3) we assume that the position of neutral axis is fixed (i.e. k is constant), even though with increasing curvature the neutral axis tends to shift outwards (i.e. k increases). Axial displacement, axial velocity and axial acceleration as a function of time have been qualitatively plotted in fig.9.

The velocity is discontinuous for $t = nT_f/2$ (with $n=1,2...$). In these characteristic points, the section is subjected to a vertical impulse which reverses the displacement direction, changing sign to the axial velocity. These points correspond to the crack closure and the sudden shift of the neutral axis from one side of the section to the other (as depicted in fig.9). These impulses are the main cause of the vertical oscillations observed in the analyses. Outside these points, the section is still subjected to a vertical acceleration as the result of the flexural response. This component of the acceleration, smaller than the impulsive one at bending reversal, is found as the second derivative of (3). Its maximum value is :

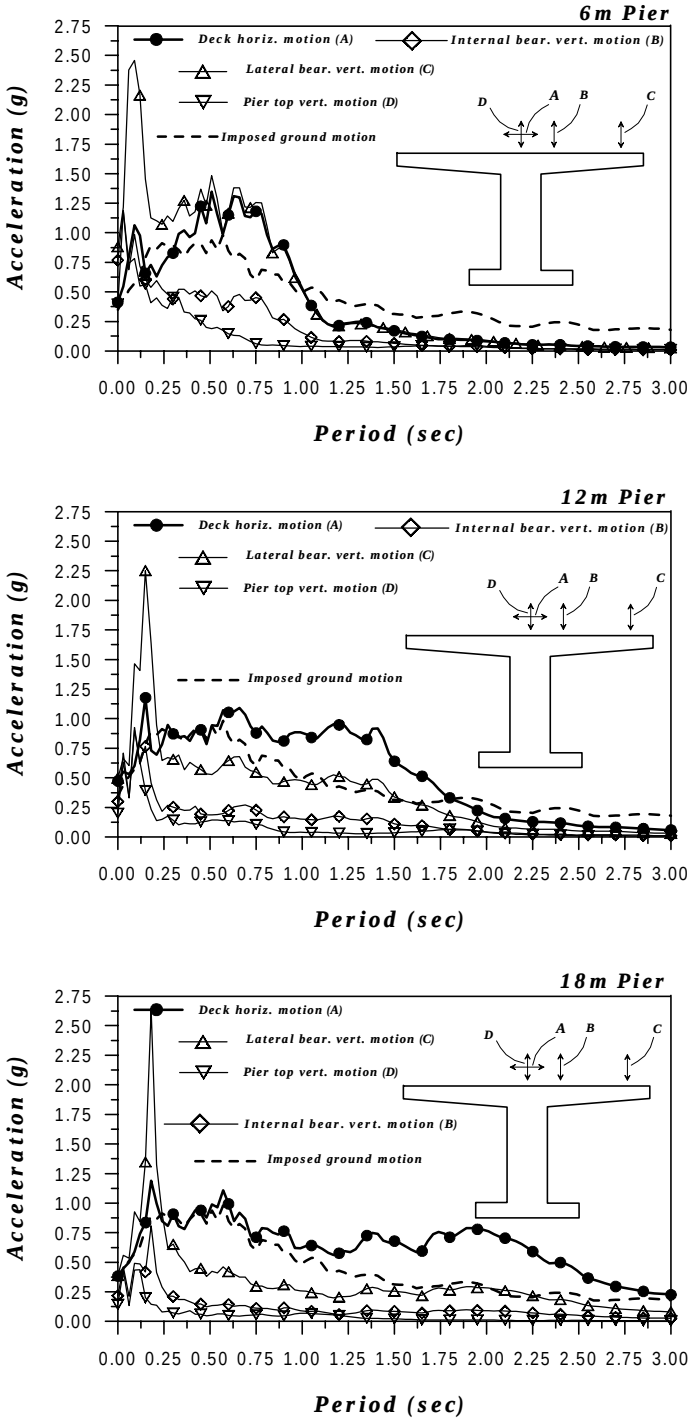

Figure 8 – Accelration Response spectra on the deck

$$\left[a^{max}\right]_{\left(t\neq n\frac{T_f}{2}\right)}=\left[\left(\frac{d^2\varepsilon_p}{dt^2}\right)^{max}\right]_{\left(t\neq n\frac{T_f}{2}\right)}=\chi^{max}\frac{4\pi^2}{T_f^2}\left(k-\frac{1}{2}\right)d \qquad (4)$$

This component of the vertical acceleration is negligible when compared to that due to the impulse at bending reversal (see eq.(7)).

In order to obtain an estimate for the magnitude of this impulse, the assumption of rigid body motion must be relaxed and the impact at crack closure treated as an elastic rebound. We assume therefore that this elastic impact takes place in a finite time interval Δt.

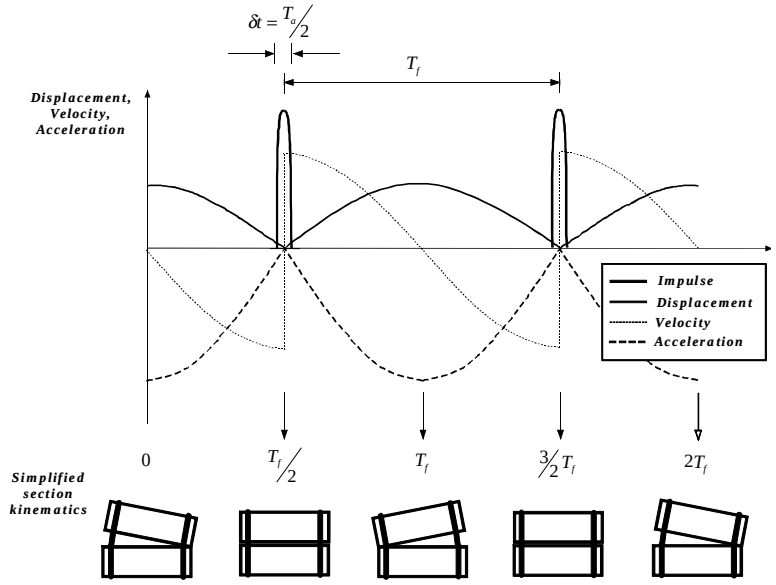

Figure 9 – Section kinematics

With these hypotheses, the impulse amplitude can be computed as:

$$m\Delta v = \int_{\Delta t} f\,dt = \int_{\Delta t} m\,a\,dt \qquad (5)$$

where m is the mass and f the inertia force. The velocity variation Δv that takes place during the time interval Δt can be set according to Fig.9 by computing the right and left limit of the first derivative of (3) for $t \rightarrow nT_f/2$. The time interval Δt is tentatively set equal to one half the fundamental axial period of the pier-deck system ($\Delta t = T_a/2$), so that Δt corresponds to the compressive semi-cycle of the pier elastic rebound. Therefore, the velocity variation within the specified time interval is :

$$\Delta v = 2\left[\frac{d\varepsilon_p}{dt}\right]_{\left(t\rightarrow n\frac{T_f}{2}\right)}=2\chi^{max}\frac{2\pi}{T_f}\left(k-\frac{1}{2}\right)d \qquad (6)$$

If we assume that the impulse has a sinusoidal shape, we obtain from (5):

$$\left[a^{max}\right]_{\left(t=n\frac{T_f}{2}\right)}=\frac{\pi}{2}\frac{\Delta v}{\Delta t}=\frac{\pi}{2}\frac{2}{T_a}\chi^{max}\frac{4\pi}{T_f}\left(k-\frac{1}{2}\right)d \qquad (7)$$

where the $\pi/2$ factor is found by integrating the sinusoidal impulse over the time interval Δt in (5).

A simple relation between the pier maximum horizontal acceleration response and the curvature maximum acceleration can be easily obtained by assuming the flexural deformations taking place in a localised plastic hinge at the column base. In this case we obtain that the maximum acceleration at pier top is :

$$a_h=\beta(T_f)=l_{cp}H\left(\frac{d^2\chi}{dt^2}\right)^{max}=l_{cp}H\chi^{max}\frac{4\pi^2}{T_f^2} \qquad (8)$$

where l_{cp} is the plastic hinge length, H the pier height and $\beta(T_f)$ is the ordinate of the acceleration response spectrum for the pier predominant flexural period. The simplification associated with this kinematic mechanism is valid for single column bents in general and also for members that tend to oscillate in double bending, because maximum curvature at column base is, in most cases, one order of magnitude greater than that at column top, where yielding of steel seldom occurs.

Similarly, if the largest axial deformations take place within the plastic hinge region, as it is for the plastic rotations, the maximum value of the impulsive $(a_{v,i})$ component of the pier vertical acceleration can be written as:

$$a_{v,i}=l_{cp}\left[\left(\frac{d^2\varepsilon_p}{dt^2}\right)^{max}\right]_{\left(t=n\frac{T_f}{2}\right)}=\left(\frac{T_f}{T_a}\right)\beta(T_f)\left(k-\frac{1}{2}\right)\frac{d}{H} \qquad (9)$$

A comparison between the values found with eq.(9) and the results of the non-linear analyses for the rigid deck model are presented in the following table 3. Horizontal and vertical accelerations found from time-history analyses are indicated with β_h and β_v respectively. The flexural period of the piers T_f has been calculated by using the secant flexural stiffness at maximum response (average stiffness). The axial period T_a instead has been computed using the cracked elastic stiffness and the neutral axis depth evaluated at maximum response. In this case study, both secant stiffness and neutral axis depth, were available from the results of the non-linear analyses; for design purpose instead, they should be calculated by using the assumed structural ductility or the maximum expected displacement, if a displacement based design approach is being used.

Tab. 4 - Numerical analysis versus Eq.(9) prediction

Pier Height	β_h	β_v	T_a [sec]	T_f [sec]	(k -1/2)	$a_{v,i}$	$\beta_v / a_{v,i}$
6	4.12	3.96	0.10	0.69	0.27	3.19	1.24
12	4.72	2.00	0.13	1.21	0.22	2.0	1.00
18	3.83	1.43	0.15	1.92	0.18	1.22	1.17

The results from table 4 seem to indicate the soundness of the assumptions used to derive equation (9) and the capability of it to provide a correct estimate of the magnitude of these axial vibrations.
From the cases presented above it seems that little or no amplification of the axial motion is found between pier base and pier top. However, it is important to note that the axial input found with (9) might have been overestimated due to the assumption of section rigid body motion.
Results obtained with eq.(9) are strongly affected by the value assumed for $\beta_h(T_f)$. In our case this value was given by the results of non linear time history analyses (β_h), whereas in design it must be found from a design spectrum based on the maximum expected ductility (i.e. behaviour factor).

CONCLUSIONS

Although experimental results are needed to confirm the predictions of the numerical study presented herein, there is no doubt that a significant contribution to the vertical acceleration in RC piers subjected to seismic excitation is due to the rocking mechanism. This contribution is neglected in ordinary design, based on linear modal analysis and response spectra. The intensity of this vertical acceleration may in effect be greater than the structural response to the vertical component of the seismic input motion. The effect of this additional motion in the vertical direction can be particularly severe on deck bearings, which may experience the maximum horizontal shear forces associated with very low vertical reactions providing an additional explanation for the widespread phenomenon of bearing failure and deck unseating observed during past earthquakes.
Based on the preliminary investigations presented herein, it seems that equation (9) provides a reasonable estimate of the vertical accelerations in bridge piers subjected to horizontal seismic input motion alone. This equation could be used as a starting point towards the definition of a design formula for the quantification of this additional vertical component to be used in the dimensioning of bridges in seismic areas.

REFERENCES

Elnashai, A.S., Papazoglou, A.J. (1997), “Procedure and Spectra for Analysis of RC Structures Subjected to Strong Vertical Earthquake Loads”, Journal of Earthquake Engineering Vol.1 n.1 , pp. 121-155, Imperial College Press.

Mander, J.B., Priestley, M.J.N., and Park, R. (1988). "Theoretical Stress-Strain Model for Confined Concrete." *Journal Struct. Eng.*, ASCE, 114(8), 1804-1826.

Menegotto, M. and Pinto, P.E. (1977). "Slender RC Compressed Members in Biaxial Bending." J.Struct. Engrg, ASCE, 103(3), 587-605.

Ono, K., Kasai, H., Sasagawa, M. (1996), “Up-down Vibration Effects on Bridge Piers”, Special is sue of Soils and Foundations, Japanese Geothecnical Society, pp. 211-218.

Papazoglou, A.J., Elnashai, A.S., (1996), “Analytical and Field Evidence of the Damaging Effect of Vertical Earthquake Ground Motion”, Earthquake Engineering and Structural Dynamics, Vol.25., pp.1109-1137.

Petrangeli, M. and Pinto, P.E. (1997). "Finite Element Modelling of the Hanshin Viaduct Failure in Kobe."*Proc. of the Second Japan-Italy Workshop on Seismic Design of Bridges,* Rome,Italy.

Petrangeli, M,. Pinto, P.E. and Ciampi, V. (1999). "A Fibre Beam Element for cyclic bending and shear. Part I and II", J. Mech. Engrg., ASCE,